

lengths. However, the present paper shows that free draining is important for short PDMS chains and that the impermeable behavior of POE is confirmed as being due to strong polymer-solvent interactions.<sup>15,17</sup> The friction coefficient per segment,  $\zeta$ , for PDMS has also been shown to vary with chain length and solvent in a manner similar to that found previously<sup>15</sup> for PM.

The deviations from Kirkwood-Riseman theory for PM and PDMS at short chain lengths probably originates in the assumptions of point centers of friction and a solvent continuum. However modification of the Oseen tensor to account for finite segment sizes cannot explain the observed variation of  $\zeta$  with solvent. Hence, one is forced to conclude that solvent structure must be taken into account in some way, and, in the absence of improved hydrodynamic theories, semiempirical correlations provide a reasonable rationale of such behavior.

**Acknowledgment.** C.J.C.E. and D.R. gratefully acknowledge financial support from the Science Research Council. We thank Dr. J. A. Semlyen (University of York) for providing the PDMS samples.

## References and Notes

- (1) Kirkwood, J. G. *J. Polymer Sci.* **1954**, *12*, 1.
- (2) Kaye, A.; Stepto, R. F. T., unpublished work.
- (3) Kirkwood, J. G.; Riseman, J. *J. Chem. Phys.* **1948**, *16*, 565.
- (4) Oseen, C. W. "Hydrodynamik"; Akademisches Verlag: Leipzig, 1927.
- (5) Burgers, J. M. "Second Report on Viscosity and Plasticity", Amsterdam Academy of Sciences; Nordemann Publishing Co.: Amsterdam, 1938; Chapter 3.
- (6) Yamakawa, H. "Modern Theory of Polymer Solutions"; Harper and Row: London, 1971; Section 32.
- (7) Zimm, B. H. *Macromolecules* **1980**, *13*, 592.
- (8) Burchard, W.; Schmidt, M. *Macromolecules* **1981**, *14*, 210.
- (9) Fixman, M. *Macromolecules*, in press.
- (10) Dewan, R. K.; van Holde, K. E. *J. Chem. Phys.* **1963**, *39*, 1820.
- (11) Paul, E.; Mazo, R. M. *J. Chem. Phys.* **1968**, *48*, 1405.
- (12) Jain, D. V. S.; Tewari, K. K. *Chem. Phys. Lett.* **1971**, *10*, 487.
- (13) Hill, J. L.; Stepto, R. F. T. *Proc. IUPAC Int. Symp. Macromol. Helsinki* **1972**, *3*, 325.
- (14) Freire, J. J.; Horta, A. *J. Chem. Phys.* **1976**, *65*, 4049.
- (15) Mokrys, I. J.; Rigby, D.; Stepto, R. F. T. *Ber. Bunsenges. Phys. Chem.* **1979**, *83*, 446.
- (16) Edwards, C. J. C.; Stepto, R. F. T.; Semlyen, J. A. *Polymer* **1980**, *21*, 781.
- (17) Couper, A.; Stepto, R. F. T. *Trans. Faraday Soc.* **1969**, *65*, 2486.
- (18) Flory, P. J.; Crescenzi, V.; Mark, J. E. *J. Am. Chem. Soc.* **1964**, *86*, 146.
- (19) Mark, J. E.; Flory, P. J. *J. Am. Chem. Soc.* **1965**, *87*, 1415.
- (20) Abe, A.; Jernigan R. L.; Flory, P. J. *J. Am. Chem. Soc.* **1966**, *88*, 631.
- (21) Lal, M.; Turpin, M. A.; Richardson, K. A.; Spencer, D. *ACS Symp. Ser.* **1975**, No. 8, 16.
- (22) Lal, M.; Stepto, R. F. T. *J. Polym. Sci., Polym. Symp.* **1977**, No. 61, 401.
- (23) Stepto, R. F. T. Ph.D. Thesis, University of Bristol, 1962.
- (24) Mokrys, I. J. Ph.D. Thesis, University of Manchester, 1976.
- (25) Schulz, G. V.; Haug, A. Z. *Phys. Chem. (Frankfurt/Main)* **1962**, *34*, 328.
- (26) Haug, A.; Meyerhoff, G. *Makromol. Chem.* **1962**, *53*, 91.

## On the Conformation of Peptides in Solution. Circular Dichroism Studies of *N*-Acetyl-L-alanine *N*-Methylamide and *N*-Acetyl-L-serine *N*-Methylamide

Joseph M. Dungan, III, and Thomas M. Hooker, Jr.\*

Department of Chemistry, University of California, Santa Barbara, California 93106.  
Received March 31, 1981

**ABSTRACT:** The simplest model compounds which include the primary structural elements of polypeptides are the *N*-methylamides of *N*-acetyl- $\alpha$ -amino acids. The conformation of such compounds has been the subject of extensive experimental and theoretical study. In the present investigation, an origin-independent matrix formalism has been used to calculate rotatory strengths for *N*-acetyl-L-alanine *N*-methylamide and *N*-acetyl-L-serine *N*-methylamide as a function of conformation. In an attempt to place limits on the nature of the conformers which are present in solution, the calculated rotatory strengths were compared with circular dichroism spectra which were measured under various experimental conditions. The results of this investigation indicate that many of the conformational energy calculations which have been reported in the literature seem to yield a reasonable representation of the conformation assumed by these molecules in nonpolar, but not polar media.

## Introduction

Historically, the conformation of proteins and polypeptides has been an important area of research, with the dipeptide model playing a pivotal role. Recent work in this laboratory has been directed toward the calculation of the optical properties of proteins and polypeptides as an aid to the study of macromolecular conformation in solution. As an adjunct to such studies, it has proven useful to investigate simple model systems which simulate the interactions responsible for the specialized properties of macromolecules. Among the simplest compounds which include the essential structural elements of a polypeptide backbone are the *N*-methylamides of *N*-acetyl amino acids.

These compounds have been the subject of extensive theoretical analyses by a variety of conformational energy methods,<sup>1-24</sup> which have indicated that their preferred conformational states can be described with the aid of a limited number of spatial forms. However, there has been disagreement as to the number and exact nature of these species.

The preferred conformational state of these compounds in solution has also been the subject of numerous experimental studies utilizing techniques such as infrared spectroscopy,<sup>23,25-35</sup> proton nuclear magnetic resonance spectrometry,<sup>24,25-27,36,37</sup> Raman spectroscopy,<sup>38,39</sup> measurement of dipole moment,<sup>40,41</sup> ultraviolet absorption

spectroscopy,<sup>42</sup> and measurement of optical activity.<sup>42–48</sup> In many of these investigations the presence of two spatial forms in equilibrium has been suggested. However, there has not been general agreement as to the specific geometry of the proposed conformers.

Circular dichroism (CD) is among the most sensitive of the physical techniques which are commonly used for the study of molecular conformation in solution. The CD of chromophores which are inherently symmetric depends directly upon the relative orientations of the molecular groups; i.e., it is dependent upon the interactions among the groups and, therefore, upon molecular geometry. Thus, it is an ideal method for investigating the nature of the conformers existing in solution. Furthermore, the amide chromophore is relatively well characterized in regard to its optical parameters, allowing for the calculations of its spectroscopic properties as a function of conformation. Thus, the comparison of experimentally derived CD spectra with theoretical chiroptical calculations should be useful for the investigation of the conformation of these compounds in solution.

Bayley, Nielsen, and Schellman<sup>49</sup> carried out a pioneering investigation into the dependence of the optical properties of dipeptides upon conformation. The present investigation is similar to theirs in several respects; for example, the theoretical formalism is a matrix-based configuration interaction method and similar optical parameters have been employed. However, there are also important differences between this study and the earlier work. The present theoretical formalism, although derived directly from that of Bayley et al., is significantly different. Furthermore, this study is directed specifically at the *N*-methylamides of *N*-acetyl amino acids. In addition, static charges are distributed over all the atoms of each molecule in the present calculations, whereas Bayley et al. considered only those atoms directly associated with the amide chromophore, which might lead to differences insofar as the calculated chiroptical properties of the  $n-\pi^*$  transitions are concerned.

The model compounds studied in the present work were *N*-acetyl-L-alanine *N*-methylamide (NALANMA) and *N*-acetyl-L-serine *N*-methylamide (NALSNA). The general procedure was to compute the optical properties as a function of conformation. These theoretical results were compared with experimental absorption and CD data to obtain information as to the conformations assumed by these molecules in solution and as a means for testing the results of various conformational energy methods.

## Experimental Section

*N*-Acetyl-L-alanine *N*-methylamide (NALANMA) was obtained from Vega-Fox Chemical Co. as a white crystalline solid and used without further purification. No extraneous absorption bands were detected in the ultraviolet spectrum. The prominent bands which were observed in the infrared spectrum were those expected. The compound gave one spot when subjected to thin-layer chromatography on silica gel with 4:1:1 butanol-acetic acid-water, visualized with iodine. The melting point was 175–176 °C (lit.<sup>23,50</sup> mp 175–176 °C). The mass spectrum showed no evidence of molecules with molecular weights greater than that of NALANMA ( $m/e$  144).

*N*-Acetyl-L-serine *N*-methylamide (NALSNA) was obtained from Vega-Fox Chemical Co. as a white crystalline solid and was used after successive recrystallizations from methanol-ether and acetone-ether. The original product showed two spots in thin-layer chromatography on silica gel with 4:1:1 butanol-acetic acid-water, visualized with iodine. Furthermore, a band centered near 280 nm was observed in the absorption spectrum. After recrystallization the compound gave one spot when subjected to thin-layer chromatography and there was no extraneous absorption band in the UV spectrum. The prominent bands in the

infrared spectrum were those expected. The melting point was 115–116 °C (lit.<sup>23,51</sup> mp 117 °C). The mass spectrum gave a pattern consistent with the compound being authentic ( $m/e$  160).

The solvents used were spectrograde dioxane, acetonitrile, cyclohexane (all from Matheson Coleman and Bell), and triethyl phosphate (TEP), which was obtained from Aldrich Chemicals and distilled under reduced pressure. All aqueous solutions were prepared with distilled, deionized water which was saturated with nitrogen. Dioxane was passed through alumina and stored under nitrogen until used.

Solutions were made up by weighing the solute directly into volumetric flasks. All solutions, except those in TEP, were filtered through a Millipore apparatus immediately prior to spectral measurements. TEP solutions were filtered through sintered glass.

UV absorption spectra were obtained by means of a Cary 118C recording spectrophotometer equipped with the Cary far-UV modification. All absorption spectra were measured at ambient temperature using fused silica cells with path lengths of 1.0 and 0.1 cm.

CD spectra were measured on a dichrograph based upon a Cary 60 recording spectropolarimeter. The instrument is equipped with an end-on photomultiplier tube and a 50-kHz modulation system. Spectra were determined at 27 °C using fused silica cells with path lengths between 0.05 and 1.0 cm. Spectra were also measured at –48 °C in ethanol solution. The data were acquired with the aid of a PDP-11/GT-40 digital computer system which allowed multiple scanning and signal averaging. All CD data reported herein are the combination of at least four separate runs of up to 25 scans each. The data are reported as molar ellipticities,  $M_\theta$ , which is defined as

$$\theta = M_\theta(Cl/100)$$

where  $\theta$  is the observed ellipticity,  $l$  is the path length in cm, and  $C$  is the solute concentration in moles per liter.

## Theoretical Methods

The theoretical optical calculations carried out in this investigation were by means of a matrix-based independent-systems formalism, which includes configuration interaction between excited states. The formalism is essentially an origin-independent variant of the matrix method that has been described by Bayley et al.<sup>49</sup> The most significant difference between the present method and that of Bayley et al. is that the calculations are carried out in the momentum rather than the dipole moment representation.<sup>52</sup> All of the common mechanisms which are usually considered to be involved in the generation of optical activity by the interaction of molecular groups are implicit in this theoretical formalism.

In order to carry out calculations as a function of conformation, one must know the geometry of the molecule under study. In addition, one must know the energies of the various electronic transitions, the directions and magnitudes of the transition moments, and the static charges associated with the atoms of the molecule. If the calculations are to be performed in the distributed monopole approximation,<sup>53</sup> the charge monopoles associated with transitions to the excited states must be known as well.

The peptide chromophore has been extensively studied and is known to possess at least two electronic transitions above 185 nm, an electronically allowed  $\pi-\pi^*$  transition, which occurs near 188 nm in the monomer, and a magnetically allowed  $n-\pi^*$  transition, which occurs from 212 to 230 nm, depending upon the solvent used. The parameters for the  $\pi-\pi^*$  transitions were derived from the data of Nielsen and Schellman,<sup>54</sup> assuming polarizations determined in the polarized absorption studies of Peterson and Simpson.<sup>55</sup> Values for the monopoles associated with the transitions were obtained from the work of Bayley et al.<sup>49</sup> Data required for the  $n-\pi^*$  transitions were obtained

Table I  
Calculated Atomic Coordinates and Static Charges for  
NALANMA and NALSNNMA in the  
Fully Extended Conformation

| atom                        | x      | y      | z       | Q <sub>ALA</sub> | Q <sub>SER</sub> |
|-----------------------------|--------|--------|---------|------------------|------------------|
| C <sub>1</sub> <sup>α</sup> | 0.000  | 0.000  | 0.000   | 0.0463           | 0.0590           |
| C <sub>1</sub> <sup>β</sup> | -0.511 | -1.439 | 0.000   | 0.3180           | 0.3190           |
| C <sub>1</sub> <sup>γ</sup> | -0.514 | 0.726  | -1.257  | -0.1100          | 0.0417           |
| H <sub>1</sub> <sup>α</sup> | -0.356 | 0.503  | 0.875   | 0.0457           | 0.0472           |
| H <sub>1</sub> <sup>β</sup> | 1.878  | -0.913 | 0.000   | 0.2040           | 0.2040           |
| H <sub>1</sub> <sup>γ</sup> | -1.069 | 0.0976 | -1.8013 | 0.0399           | 0.0524           |
| H <sub>2</sub> <sup>β</sup> | -1.069 | 1.5118 | -0.984  | 0.0399           | 0.0524           |
| H <sub>3</sub> <sup>β</sup> | 0.2637 | 1.041  | -1.8018 | 0.0399           |                  |
| H <sub>3</sub> <sup>γ</sup> | 1.4123 | 0.9218 | -1.5954 |                  | 0.302            |
| O <sub>1</sub> <sup>γ</sup> | 0.290  | -2.397 | 0.000   | -0.422           | -0.421           |
| O <sub>1</sub> <sup>β</sup> | 0.5981 | 1.1762 | -2.0358 |                  | -0.457           |
| N <sub>1</sub>              | 1.467  | 0.000  | 0.000   | -0.202           | -0.200           |
| C <sub>0</sub>              | 2.188  | 1.109  | 0.000   | 0.313            | 0.313            |
| C <sub>0</sub>              | 3.698  | 0.873  | 0.000   | -0.0978          | -0.0978          |
| H <sub>0</sub> <sup>1</sup> | 4.100  | 1.286  | -0.817  | 0.0419           | 0.0419           |
| H <sub>0</sub> <sup>2</sup> | 4.101  | 1.287  | 0.816   | 0.0419           | 0.0419           |
| H <sub>0</sub> <sup>3</sup> | 3.882  | -0.110 | 0.001   | 0.0419           | 0.0419           |
| O <sub>0</sub>              | 1.721  | 2.258  | 0.000   | -0.422           | -0.422           |
| C <sub>2</sub>              | -2.514 | -2.851 | 0.000   | -0.0648          | -0.0648          |
| H <sub>2</sub> <sup>1</sup> | -3.502 | -2.699 | 0.014   | 0.0474           | 0.0474           |
| H <sub>2</sub> <sup>2</sup> | -2.244 | -3.375 | 0.808   | 0.0474           | 0.0474           |
| H <sub>2</sub> <sup>3</sup> | -2.269 | -3.360 | -0.825  | 0.0474           | 0.0474           |
| H <sub>2</sub>              | -2.432 | -0.767 | 0.000   | 0.204            | 0.204            |
| N <sub>2</sub>              | -1.820 | -1.556 | 0.000   | -0.200           | -0.200           |

<sup>a</sup> H<sub>3</sub><sup>β</sup> occurs only in NALANMA. <sup>b</sup> H<sup>γ</sup> and O<sup>γ</sup> occur only in NALSNNMA.

Table II  
UV Absorption Data<sup>a</sup>

| solvent          | N-acetyl-L-alanine<br>N-methylamide |                      |      | N-acetyl-L-serine<br>N-methylamide |                      |      |
|------------------|-------------------------------------|----------------------|------|------------------------------------|----------------------|------|
|                  | λ <sub>max</sub>                    | ε × 10 <sup>-3</sup> | Δ    | λ <sub>max</sub>                   | ε × 10 <sup>-3</sup> | Δ    |
| H <sub>2</sub> O | 187.2                               | 15.3                 | 14.2 | 187.5                              | 14.4                 | 14.3 |
| acetonitrile     | 187.6                               | 13.2                 | 14.6 | 187.7                              | 13.6                 | 14.7 |
| TEP              | 188.5                               | 13.5                 | 14.7 | 188.5                              | 13.9                 | 15.2 |

<sup>a</sup> Wavelengths are in nanometers.

from the works of Bayley et al. and Schellman and Nielsen.<sup>56</sup>

The atomic coordinates for NALANMA and NALSNNMA were based on the crystal structures of *N*-acetyl-glycine,<sup>57</sup> *L*-serine monohydrate,<sup>58</sup> and *L*-alanine,<sup>59</sup> with hydrogen atoms added assuming standard bond lengths and angles. Significant structural distortions were corrected to idealized values.<sup>60</sup> The dihedral angles,  $\phi$ ,  $\psi$ , and  $\chi^i$ , have been defined according to the standard conventions.<sup>61</sup> Both the C- and N-terminal methyl hydrogen atoms were fixed in the staggered position. The atomic coordinates for NALANMA and NALSNNMA in the extended conformation are presented in Table I.

The total static charge on each atom, which is also given in Table I, is the sum of  $\sigma$  and  $\pi$  contributions. These static charges were obtained from the work of Poland and Scheraga,<sup>62</sup> which was based upon the MO-LCAO method of Del Re, Pullman, and co-workers.<sup>63-66</sup>

The choice of a value for the effective dielectric constant can influence the theoretical optical calculations. In the present case a constant value of 2 has been assumed.

All computations were carried out on IBM 360/75 and ITEL AS/6 digital computers at the University of California, Santa Barbara Computer Center.

## Experimental Results

Absorption data for NALANMA and NALSNNMA are summarized in Table II. These data represent an average of four runs of each spectrum utilizing different concen-

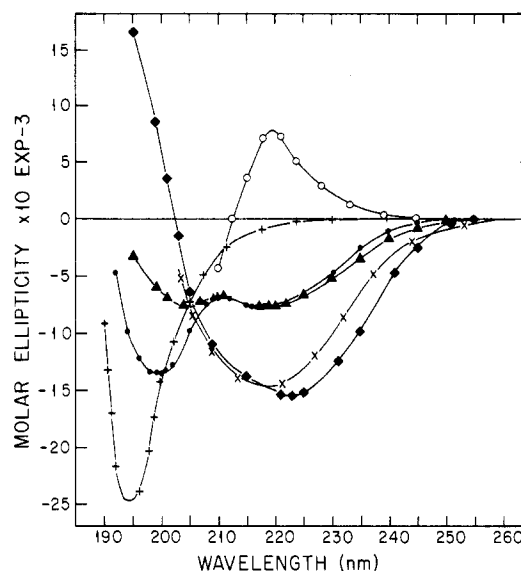


Figure 1. Circular dichroism spectra at 27 °C for *N*-acetyl-L-alanine *N*-methylamide in water (+), acetonitrile (●), triethyl phosphate (▲), dioxane (×), and cyclohexane (◆) and at -48 °C for ethanol (○). The data obtained at -48 °C in ethanol have been multiplied by a factor of 10.

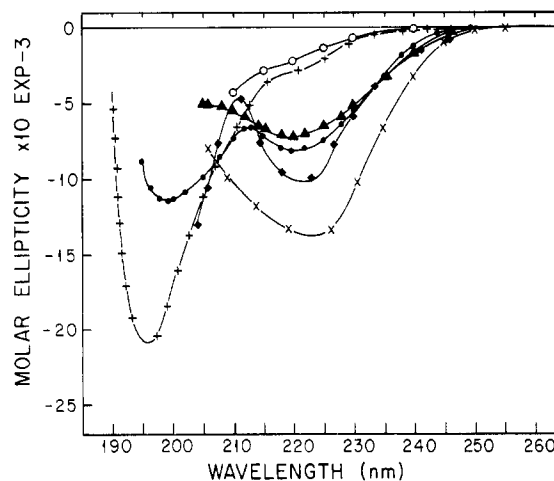
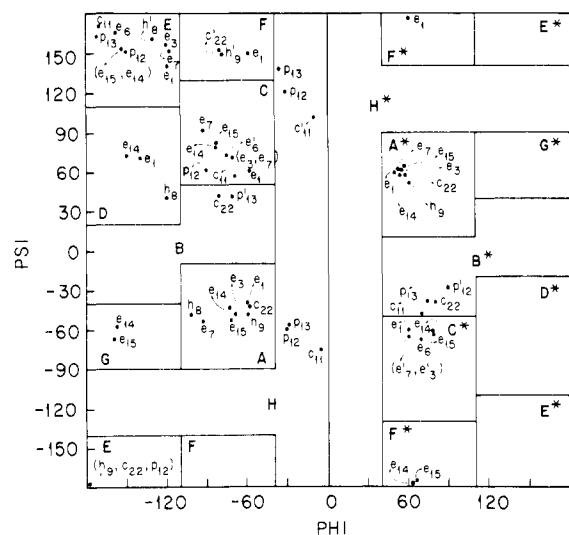


Figure 2. Circular dichroism spectra at 27 °C for *N*-acetyl-L-serine *N*-methylamide in water (+), acetonitrile (●), triethyl phosphate (▲), dioxane (×), and 9:1 (v/v) cyclohexane-triethyl phosphate (◆) and at -48 °C for ethanol (○).

trations and path lengths. The UV absorption studies showed a single significant peak above 180 nm, the position, shape, and magnitude of which varied with the solvent. The observed UV spectra for NALANMA are in agreement with spectra reported previously by others.<sup>42,54</sup>

The CD spectra of NALANMA in various solvents are shown in Figure 1. They reveal at least two electronic transitions in all the solvents which permitted penetration to sufficiently short wavelengths. The sign, shape, position, and intensity, especially in the case of the longer wavelength band, varied with solvent. The sign of this band was also sensitive to temperature; it was clearly positive at -48 °C whereas it was apparently very weakly negative at 27 °C. Although the band obviously gives rise to a positive Cotton effect at low temperatures, extensive efforts to curve fit the aqueous solution spectrum determined at 27 °C with a positive Cotton effect in this wavelength region proved futile. A satisfactory fit could be obtained only with a very weak negative band. The CD results for NALANMA are in essential agreement with similar studies by other investigators.<sup>42-48</sup>



**Figure 3.**  $\phi$ - $\psi$  map for *N*-acetyl-L-alanine *N*-methylamide summarizing the results of conformational energy calculations by various workers. Lower case letters indicate the type of conformational energy method as follows: e = empirical, h = EHT, c = CNDO, p = PCILO. Numerical subscripts denote citations to literature from which data were obtained. See text for definitions of other symbols used.

The CD spectra of NALSNMA in various solvents are reported in Figure 2. The lower wavelength band underwent no changes in sign, but it did exhibit an apparent blue shift with increasing solvent polarity. The longer wavelength band, which was also negative, showed a decrease in intensity with an accompanying blue shift as the solvent polarity increased.

The effect of variations in solute concentration upon both CD and absorption spectra was investigated for both molecules in all of the solvent systems which were utilized. Concentrations from 0.0005 to 0.002 M were investigated, although both extremes could not be attained for all of the solvent systems. However, in no case was any measurable concentration dependence observed, which can be taken to imply that there is no significant aggregation over the concentration ranges employed. This results in agreement with the gas-liquid osmometry solute association studies performed by Efremov and co-workers.<sup>67</sup>

### Theoretical Results

Numerous investigators have carried out a large number of conformational energy calculations for these model compounds by a variety of methods. In addition to empirical calculations of the hard-sphere type, partitioned potential energy function (PPE) methods, and calculations from the empirical conformational energy program for peptides (ECEPP),<sup>1-7,14-16,23</sup> a number of molecular orbital calculations have appeared. These include the extended-Hückel (EHT),<sup>8-10,17,22</sup> complete neglect of differential overlap (CNDO),<sup>11,17</sup> and perturbation configuration interaction over localized orbital (PCILO)<sup>12,13,18-21</sup> methods.

The results of various types of conformational energy calculations for NALANMA and NALSNMA, which have emanated from several laboratories, are summarized in Tables III and IV. These results are also illustrated graphically in Figures 3 and 4, where the procedure of Zimmerman et al.<sup>14</sup> has been employed to construct  $\phi$ - $\psi$  maps which are subdivided into regions denoted by a letter code. Conformations are then classified in terms of the regions of the  $\phi$ - $\psi$  maps in which they fall. On the left-hand side of the maps the letters denoting each region have the following significance: A denotes the region which

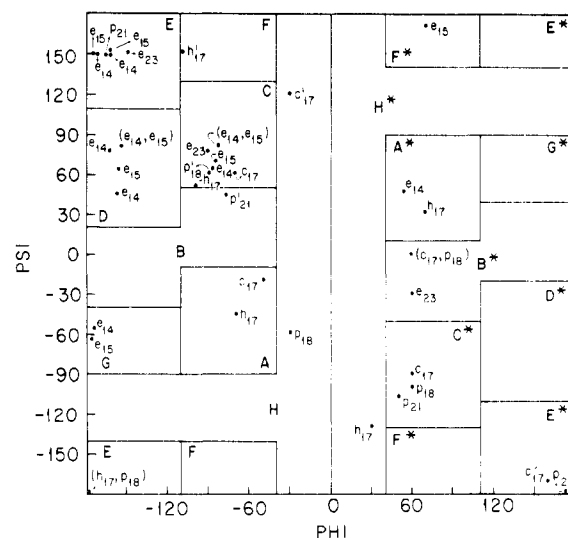


**Figure 4.**  $\phi$ - $\psi$  map for *N*-acetyl-L-serine *N*-methylamide summarizing the results of conformational energy calculations by various workers. Lower case letters indicate the type of conformational energy method as follows: e = empirical, h = EHT, c = CNDO, p = PCILO. Numerical subscripts denote citations to literature from which data were obtained. See text for definitions of other symbols used.

contains the right-handed  $\alpha$  helix, B is the bridge region, C contains the  $C_7^{eq}$  ring, which is a folded conformer with a hydrogen bond of the 3 $\rightarrow$ 1 type (third residue connected to the first) stabilizing a seven-membered ring with the side chain in the equatorial position, E contains the extended conformations such as  $C_5$ , which is a cyclic pentagonal structure stabilized by a hydrogen bond of the 1 $\rightarrow$ 1 type, and H is the high-energy region. D, F, and G are assigned to the remaining regions so as to make the maps contiguous. The regions on the right-hand half of the maps are defined by inversion of the left side through the origin and are denoted by asterisks appended to the corresponding symbols from the left-hand side. For example, A\* contains the left-handed  $\alpha$  helix and C\* contains the  $C_7^{ax}$  ring. Specific conformations within each region are denoted by points and associated letters indicating the particular conformational energy method used, the numerical subscripts denote the investigators who performed the calculations, and primes indicate global minima.

Since two transitions are included for each amide chromophore, four rotatory strengths are calculated for a dipeptide. In practice, the energies of the two  $n\text{-}\pi^*$  transitions are not split by the weak interactions which give rise to their optical rotatory power, so the  $n\text{-}\pi^*$  rotatory strengths are recorded in Tables III and IV as the sum of the two overlapping bands. Splitting of the  $\pi\text{-}\pi^*$  bands can occur as a result of the strong interactions of these transitions, giving rise to couplets, i.e., two bands of opposite sign which are split to either side of the monomer energy. The sign of a couplet is determined by the sign of its longer wavelength component; i.e., a couplet is said to be positive if its longer wavelength component is positive. Thus, only two rotatory strengths are reported for each conformer in the tables.

The calculations for species in aqueous solution were performed with transition energies for the monomers of 212 and 188 nm for the  $n\text{-}\pi^*$  and  $\pi\text{-}\pi^*$  transitions, respectively; monomer energies of 220 and 186 nm were employed for calculations dealing with nonpolar solvent systems. The results of the chiroptical calculations for aqueous solutions are reported in Figures 5 and 6, in the form of maps of nodal lines for the rotatory strength as

Table III  
Theoretical Chiroptical Results for NALANMA<sup>a</sup>

| $\phi$ , deg | $\psi$ , deg | $\chi'$ , deg | $n-\pi^*$  | low-energy $\pi-\pi^*$ | splitting | conformational letter code                            |
|--------------|--------------|---------------|------------|------------------------|-----------|---|
| -180         | -180         | 60            | -0.011 762 | 0.001 766              | 4.18      | E <sub>h9</sub> , E <sub>c22</sub> , E <sub>p12</sub> |
| -171         | 164          | 65            | -0.047 247 | -0.062 985             | 4.14      | E <sub>p13</sub>                                      |
| -170         | 170          | 60            | -0.030 302 | 0.142 647              | 4.18      | E <sub>c11</sub>                                      |
| -160         | -68          | 39            | 0.000 289  | -0.955 596             | 0.13      | G <sub>e15</sub>                                      |
| -158         | -58          | 54            | -0.003 691 | -0.636 750             | 0.70      | G <sub>e14</sub>                                      |
| -158         | 165          | 60            | -0.032 782 | 0.494 500              | 4.22      | E <sub>e6</sub>                                       |
| -154         | 153          | 58            | -0.063 300 | 0.312 573              | 4.19      | E <sub>e15</sub>                                      |
| -154         | 153          | 60            | -0.063 226 | 0.312 567              | 4.19      | E <sub>e14</sub>                                      |
| -150         | 72           | 59            | -0.088 626 | -1.654 546             | 1.05      | D <sub>e14</sub>                                      |
| -150         | 150          | 60            | -0.068 049 | 0.383 006              | 4.20      | E <sub>p12</sub>                                      |
| -135         | 65           | 60            | -0.092 400 | -1.694 467             | 1.11      | D <sub>e1</sub>                                       |
| -130         | 155          | 60            | -0.028 031 | 1.291 175              | 4.36      | E <sub>e1</sub>                                       |
| -130         | 160          | 60            | -0.012 279 | 1.419 544              | 4.32      | E <sub>h8</sub>                                       |
| -120         | 155          | 60            | -0.011 010 | 1.626 642              | 4.36      | E <sub>e3</sub>                                       |
| -117         | 150          | 60            | -0.021 749 | 1.598 167              | 4.42      | E <sub>e7</sub>                                       |
| -100         | -50          | 60            | -0.033 218 | 1.882 010              | 2.39      | A <sub>h8</sub>                                       |
| -93          | -54          | 60            | -0.038 953 | 1.979 286              | 2.45      | A <sub>e7</sub>                                       |
| -93          | 90           | 60            | -0.138 575 | 0.278 036              | 4.88      | C <sub>e7</sub>                                       |
| -90          | 60           | 60            | -0.124 268 | -0.954 181             | 3.85      | C <sub>p12</sub>                                      |
| -84          | 79           | 61            | -0.139 092 | 0.107 222              | 5.21      | C <sub>e14</sub>                                      |
| -84          | 81           | 61            | -0.138 024 | 0.198 485              | 5.22      | C <sub>e15</sub>                                      |
| -80          | 40           | 60            | -0.093 832 | -1.489 765             | 3.47      | B <sub>e22</sub>                                      |
| -80          | 150          | 60            | 0.059 274  | 2.427 289              | 3.51      | F <sub>c22</sub> , F <sub>h9</sub>                    |
| -75          | 72           | 60            | -0.137 854 | 0.113 561              | 5.76      | C <sub>e6</sub>                                       |
| -75          | 150          | 60            | 0.068 958  | 2.477 123              | 3.22      | F <sub>e1</sub>                                       |
| -74          | -45          | 61            | -0.021 157 | 2.643 117              | 2.49      | A <sub>e14</sub>                                      |
| -72          | -54          | 58            | -0.034 770 | 2.506 018              | 2.63      | A <sub>e15</sub>                                      |
| -72          | 40           | 56            | -0.095 592 | -1.431 321             | 3.72      | B <sub>p13</sub>                                      |
| -72          | 70           | 60            | -0.137 526 | 0.132 093              | 5.98      | C <sub>e3</sub> , C <sub>e7</sub>                     |
| -70          | 55           | 60            | -0.149 402 | -0.495 650             | 5.71      | C <sub>c11</sub>                                      |
| -67          | -51          | 60            | -0.029 038 | 2.616 299              | 2.53      | A <sub>e3</sub>                                       |
| -60          | -50          | 60            | -0.024 084 | 2.735 681              | 2.17      | A <sub>h9</sub>                                       |
| -60          | -40          | 60            | -0.007 570 | 2.808 278              | 1.68      | A <sub>e1</sub>                                       |
| -60          | 60           | 60            | -0.142 369 | 0.121 640              | 6.98      | C <sub>e1</sub>                                       |
| -58          | -46          | 60            | -0.016 212 | 2.783 940              | 1.83      | A <sub>c22</sub>                                      |
| -35          | 137          | 56            | 0.122 333  | 2.464 136              | 0.28      | H <sub>p13</sub>                                      |
| -30          | -60          | 60            | 0.000 161  | 2.710 07               | 0.28      | H <sub>p12</sub>                                      |
| -30          | 120          | 60            | 0.115 855  | 2.534 247              | 1.30      | H <sub>p12</sub>                                      |
| -29          | -59          | 55            | -0.014 397 | 2.601 548              | 0.02      | H <sub>p13</sub>                                      |
| -10          | 100          | 60            | 0.098 179  | -2.630 191             | 0.76      | H <sub>c11</sub>                                      |
| -5           | -75          | 60            | -0.040 948 | -2.581 503             | 1.76      | H <sub>c11</sub>                                      |
| 50           | 60           | 60            | 0.046 966  | -2.720 172             | 2.14      | A <sub>e1</sub> *                                     |
| 52           | 60           | 60            | 0.050 471  | -2.678 899             | 2.29      | A <sub>e7</sub> *                                     |
| 54           | 57           | 65            | 0.047 335  | -2.702 060             | 2.23      | A <sub>e14</sub> *                                    |
| 54           | 60           | 60            | 0.051 245  | -2.658 980             | 2.37      | A <sub>e3</sub> *                                     |
| 55           | 63           | 71            | 0.054 801  | -2.596 005             | 2.53      | A <sub>e15</sub> *                                    |
| 58           | 56           | 60            | 0.047 769  | -2.677 275             | 2.36      | A <sub>c22</sub> *                                    |
| 60           | -60          | 60            | 0.154 000  | -0.123 067             | 6.98      | C <sub>e1</sub> *                                     |
| 60           | 50           | 60            | 0.041 199  | -2.738 029             | 2.17      | A <sub>h9</sub> *                                     |
| 60           | 175          | 60            | -0.025 421 | 1.965 396              | 0.11      | F <sub>e1</sub> *                                     |
| 61           | -67          | 60            | 0.132 225  | -0.410 268             | 6.91      | C <sub>e7</sub> *, C <sub>e3</sub> *                  |
| 64           | -178         | 80            | -0.049 220 | -2.205 810             | 0.71      | F <sub>e14</sub> *                                    |
| 65           | -177         | 90            | -0.052 952 | -2.242 673             | 0.87      | F <sub>e15</sub> *                                    |
| 70           | -69          | 60            | 0.143 495  | -0.160 732             | 6.14      | C <sub>e6</sub> *                                     |
| 70           | -50          | 60            | 0.161 693  | 0.724 952              | 5.45      | B <sub>c11</sub> *                                    |
| 75           | -40          | 60            | 0.124 499  | 1.337 184              | 4.11      | B <sub>p13</sub> *                                    |
| 78           | -65          | 93            | 0.149 708  | 0.323 004              | 5.29      | C <sub>e15</sub> *                                    |
| 78           | -64          | 87            | 0.150 216  | 0.369 476              | 5.25      | C <sub>e14</sub> *                                    |
| 80           | -40          | 60            | 0.113 709  | 1.487 842              | 3.45      | B <sub>c22</sub> *                                    |
| 90           | -30          | 60            | 0.078 978  | 2.069 953              | 2.45      | B <sub>p12</sub> *                                    |

<sup>a</sup> Rotatory strengths are in Debye Bohr magnetons and splittings are in nanometers.

a function of the dihedral angles  $\phi$  and  $\psi$  with the side-chain angles held at constant values. The values of the side-chain dihedral angles used were 60° (staggered) for  $\chi^1$  of NALANMA and 60° (gauche), 180° (trans), and 300° (gauche) for  $\chi^1$  and  $\chi^2$  of NALSNMA. These particular values were selected because they are the values that have most often been used for the various conformational energy calculations which have been carried out for these molecules. Only four maps are shown for NALSNMA since, as might be expected, the calculations were rather insen-

sitive to changes in  $\chi^2$ .  $\phi$ - $\psi$  maps are shown for  $\chi^1$  values of 60°, 180°, and 300° with  $\chi^2$  held at 60°. The only instance for which any appreciable  $\chi^2$  dependence was observed was for the conformation where both  $\chi^1$  and  $\chi^2$  were 180°. Therefore, this map is also included in Figure 6. Rotatory strengths were calculated at 20° increments of  $\phi$  and  $\psi$ . The regions of conformation space that are predicted to give rise to negative  $n-\pi^*$  Cotton effects are indicated by shading lines of positive slope, whereas the regions for which a negative long-wavelength component

Table IV  
Theoretical Chiroptical Results for NALSNMA<sup>a</sup>

| $\phi$ , deg | $\psi$ , deg | $\chi^1$ , deg | $\chi^2$ , deg | $n-\pi^*$  | low-energy $\pi-\pi^*$ | splitting | conformational letter code          |
|--------------|--------------|----------------|----------------|------------|------------------------|-----------|-------------------------------------|
| -180         | -180         | 180            | 180            | 0.011 811  | -0.001 751             | 4.18      | E <sub>h17</sub> , E <sub>p18</sub> |
| -180         | -180         | 300            | 300            | -0.050 548 | 0.009 550              | 4.18      | E <sub>p18</sub>                    |
| -177         | -64          | -90            | 55             | 0.069 315  | -1.345 373             | 0.10      | E <sub>e15</sub>                    |
| -176         | 150          | -90            | 55             | -0.028 380 | -0.647 110             | 3.91      | E <sub>e15</sub>                    |
| -174         | -56          | -88            | 53             | 0.063 991  | -1.132 516             | 0.59      | G <sub>e14</sub>                    |
| -173         | 150          | -87            | 52             | -0.020 610 | -0.526 337             | 3.94      | E <sub>e14</sub>                    |
| -166         | 147          | 313            | 350            | 0.023 482  | -0.346 626             | 3.96      | E <sub>p21</sub>                    |
| -163         | 77           | -62            | -16            | -0.041 532 | -1.627 292             | 1.01      | D <sub>e14</sub>                    |
| -163         | 150          | -60            | -20            | -0.041 413 | -0.136 474             | 4.05      | E <sub>e14</sub>                    |
| -163         | 151          | -57            | -26            | -0.042 885 | -0.107 726             | 4.07      | E <sub>e15</sub>                    |
| -157         | 46           | 172            | -60            | -0.027 315 | 1.752 581              | 0.76      | D <sub>e14</sub>                    |
| -157         | 64           | 164            | -64            | -0.039 313 | -1.718 410             | 0.33      | D <sub>e15</sub>                    |
| -154         | 81           | 68             | 55             | -0.092 465 | -1.543 325             | 1.50      | D <sub>e14</sub>                    |
| -154         | 81           | 69             | 56             | -0.087 668 | -1.543 200             | 1.50      | D <sub>e15</sub>                    |
| -110         | 150          | 60             | 20             | 0.027 034  | 1.802 873              | 4.37      | F <sub>h17</sub>                    |
| -100         | 50           | 60             | 60             | -0.107 606 | -1.613 312             | 2.18      | C <sub>h17</sub>                    |
| -90          | 60           | 60             | 60             | -0.140 943 | -0.955 090             | 3.85      | C <sub>p18</sub>                    |
| -88          | 64           | 167            | -63            | -0.112 333 | -0.713 719             | 4.27      | C <sub>e14</sub>                    |
| -85          | 69           | 162            | -64            | -0.117 477 | -0.386 096             | 4.80      | C <sub>e15</sub>                    |
| -82          | 81           | 68             | 55             | -0.129 505 | 0.271 346              | 5.39      | C <sub>e14</sub>                    |
| -82          | 81           | 69             | 56             | -0.125 060 | 0.271 491              | 5.39      | C <sub>e15</sub>                    |
| -77          | 44           | 79             | 44             | -0.161 145 | -1.230 496             | 4.17      | B <sub>p21</sub>                    |
| -70          | -45          | 300            | 60             | -0.030 344 | 2.699 017              | 2.37      | A <sub>h17</sub>                    |
| -70          | 60           | 60             | 60             | -0.163 492 | -0.261 205             | 5.91      | C <sub>e17</sub>                    |
| -50          | -20          | 60             | 180            | 0.029 265  | -2.602 640             | 1.71      | A <sub>e17</sub>                    |
| -30          | -60          | 60             | 180            | -0.019 221 | 2.715 237              | 0.29      | H <sub>p18</sub>                    |
| -30          | 120          | 60             | 30             | 0.153 241  | 2.510 736              | 1.27      | H <sub>e17</sub>                    |
| 30           | -130         | 60             | 300            | 0.040 205  | -2.820 639             | 1.62      | H <sub>h17</sub> *                  |
| 50           | -107         | 55             | 331            | -0.137 891 | -2.198 680             | 4.60      | C <sub>p21</sub>                    |
| 53           | 48           | 173            | -60            | 0.035 244  | -2.780 885             | 1.60      | A <sub>e14</sub> *                  |
| 60           | -100         | 60             | 300            | -1.778 659 | -1.778 659             | 5.54      | C <sub>p18</sub> *                  |
| 60           | -90          | 60             | 300            | -0.017 859 | -1.428 511             | 6.16      | C <sub>e17</sub> *                  |
| 60           | 0            | 60             | 180            | 0.094 400  | 2.302 727              | 2.51      | B <sub>p18</sub> *                  |
| 60           | 0            | 60             | 300            | -0.048 976 | 2.382 083              | 2.47      | B <sub>e17</sub> *                  |
| 69           | 171          | 93             | -64            | -0.021 323 | -2.029 360             | 0.62      | F <sub>e15</sub> *                  |
| 70           | 30           | 320            | 320            | -0.137 959 | -2.476 126             | 0.28      | A <sub>h17</sub> *                  |
| 170          | -170         | 180            | 180            | 0.030 267  | -0.142 611             | 4.18      | E <sub>e17</sub> *                  |
| 173          | -178         | 169            | 166            | 0.010 103  | -0.236 351             | 4.18      | E <sub>p21</sub> *                  |

<sup>a</sup> Rotatory strengths are in Debye Bohr magnetons and splittings are in nanometers.

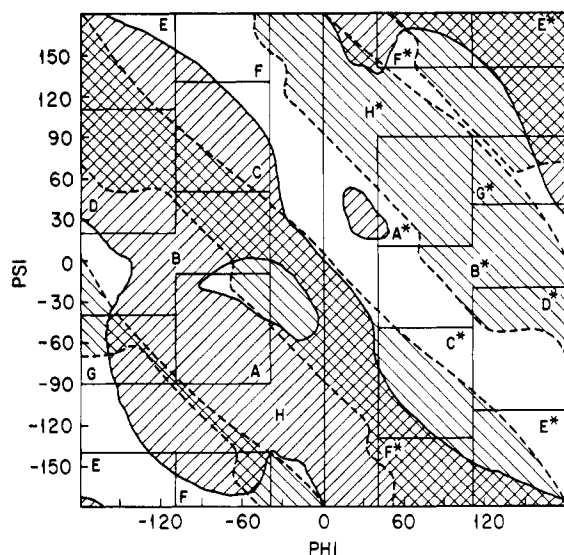


**Figure 5.** Results of chiroptical calculations for *N*-acetyl-*L*-alanine *N*-methylamide with  $\chi^1 = 60^\circ$ . Monomer energies:  $n-\pi^*$  212 nm;  $\pi-\pi^*$  188 nm.  $n-\pi^*$  nodal line (—);  $\pi-\pi^*$  nodal line (---). Shading lines of positive slope indicate negative  $n-\pi^*$  Cotton effects; lines of negative slope indicate negative  $\pi-\pi^*$  Cotton effects.

of the  $\pi-\pi^*$  couplet is calculated are indicated by shading lines of negative slope. As a result of this pattern of shading, the regions of conformation space that correspond

to conformations which predict a negative  $n-\pi^*$  with a negative  $\pi-\pi^*$  couplet are crosshatched. Regions corresponding to other possible CD patterns appear with shading of positive slope (negative  $n-\pi^*$ , positive  $\pi-\pi^*$ ), negative slope (positive  $n-\pi^*$ , negative  $\pi-\pi^*$ ), or are unshaded (positive  $n-\pi^*$ , positive  $\pi-\pi^*$ ).

The theoretical results for nonpolar solutions differ from those for aqueous solutions only slightly in terms of the intensities and energies of the Cotton effects; no differences in the signs of the bands were predicted. The positions of the nodal lines for the rotatory strengths of the nonpolar solutions were calculated to be essentially identical with those shown for the aqueous solutions.

Tables III and IV summarize the results of the chiroptical calculations for the conformers predicted to be of significance by the various conformational energy methods. Data are presented for the combined  $n-\pi^*$  bands and the longer wavelength component of the  $\pi-\pi^*$  couplets.

Figures 7 and 8 illustrate theoretical CD curves for which data characterizing the energy surface or statistical weights for significant conformers were available. These curves were calculated by assuming Gaussian bands with half-widths at  $1/e$  of maximum intensity of 12 nm and the rotatory strengths and wavelengths calculated for the conformers in either aqueous or nonpolar solvent systems as appropriate.

## Discussion

An in-depth analysis of the predictions of the various conformational energy methods, as summarized in Tables

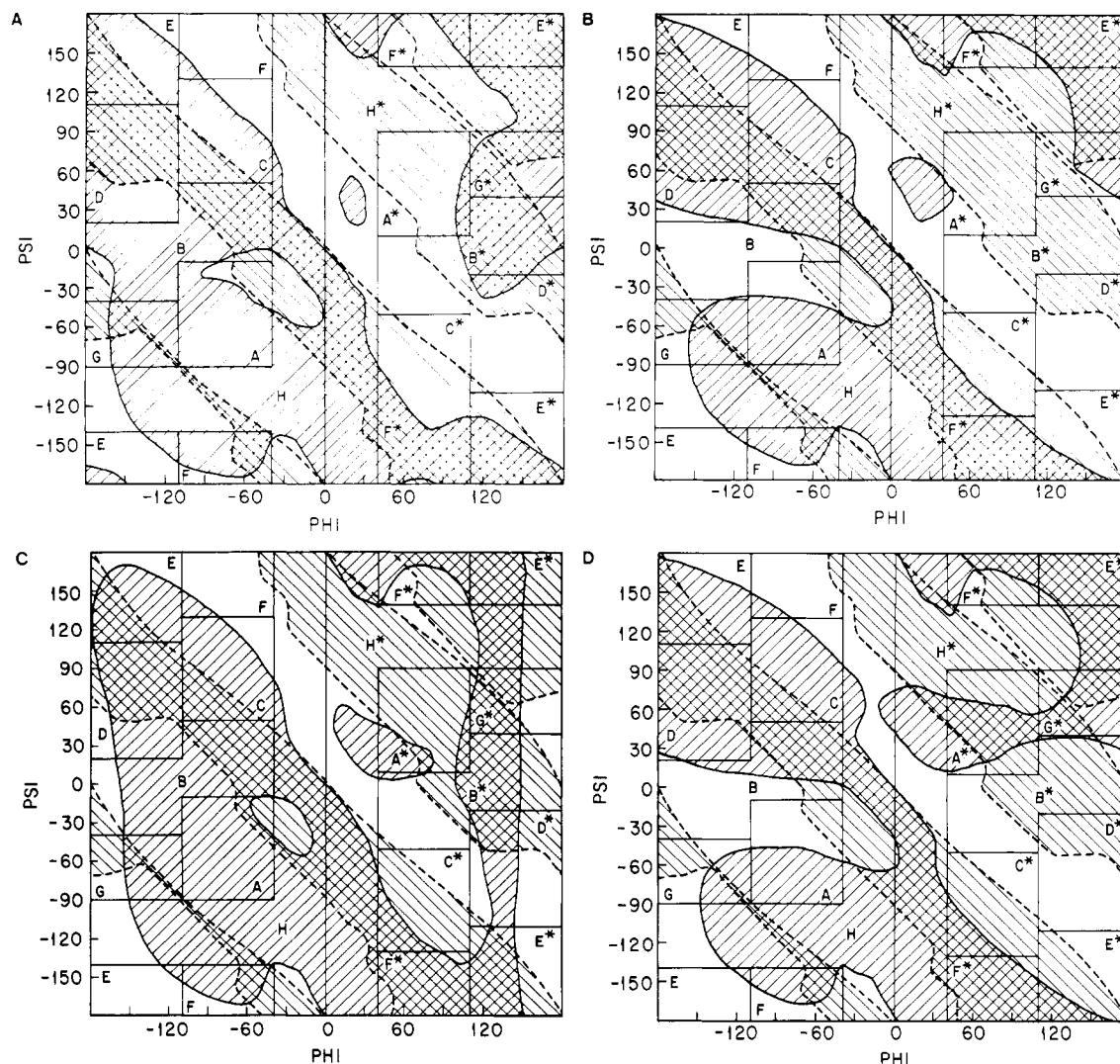


**Figure 6.** Results of chiroptical calculations for *N*-acetyl-L-serine *N*-methylamide: (A)  $\chi^1 = \chi^2 = 60^\circ$ ; (B)  $\chi^1 = 180^\circ$ ,  $\chi^2 = 60^\circ$ ; (C)  $\chi^1 = 300^\circ$ ,  $\chi^2 = 60^\circ$ ; (D)  $\chi^1 = \chi^2 = 180^\circ$ . Shaded areas indicate predicted signs of Cotton effects as in Figure 5.

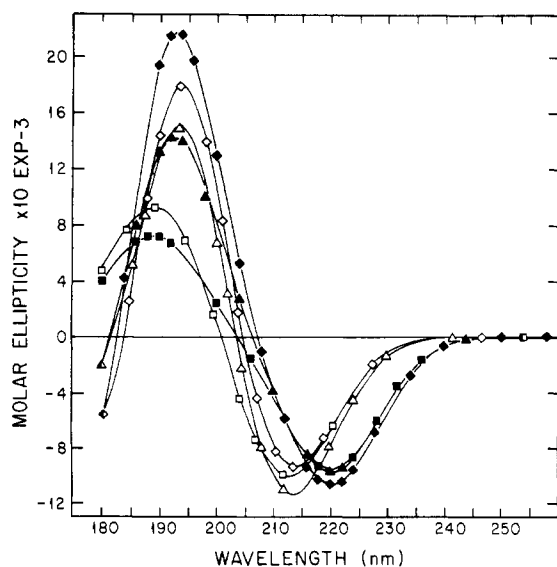


**Figure 7.** Theoretical circular dichroism curves for *N*-acetyl-L-alanine *N*-methylamide in polar (open symbols) and nonpolar (solid symbols) media. Diamonds indicate curves based on rotatory strengths which were averaged over the semiempirical energy surface determined in this work. Triangles based on data of Lewis et al.<sup>15</sup> squares based on data of Zimmerman et al.<sup>14</sup> Gaussian band shapes assumed with bandwidth of 12 nm.

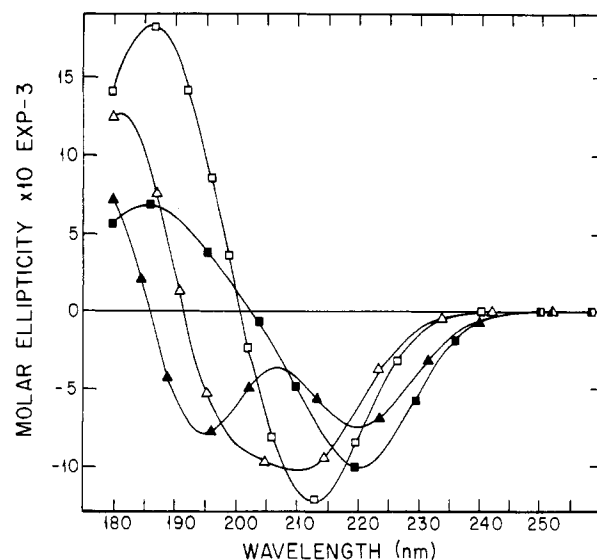


**Figure 8.** Theoretical circular dichroism curves for *N*-acetyl-L-serine *N*-methylamide in polar (open symbols) and nonpolar (solid symbols) media. Triangles were based on the data of Lewis et al.<sup>15</sup> and squares were based on the data of Zimmerman et al.<sup>14</sup>

III and IV and Figures 3 and 4, will not be presented here as several excellent reviews are available.<sup>14,15,35,68</sup> However,

from an overall point of view, it can be stated that the results as summarized here indicate that although there are similarities in the general conformational species predicted, there is considerable diversity in regard to the order of stability of various species and as to the specific values of the backbone and side-chain dihedral angles that characterize them.

The solution conformation of NALANMA and NALSNMA has been the subject of numerous experimental investigations by a variety of techniques.<sup>23–48,69,70</sup> As in the case of the conformational energy calculations, these studies have not always arrived at the same conclusions. In many cases, the existence of an equilibrium between not more than one folded ( $C_7$ ) and one extended ( $C_5$ ) conformer has been implied. However, other experimental data,<sup>29,37,40,42,47,48,69,70</sup> as well as many of the conformational energy studies cited above, suggest that there is a significant distribution of conformers in solution.

Changes in solvent can alter observed CD spectra as a result of perturbations of the energies of some electronic transitions. For a specific conformation, simple solvent shifts should lead only to apparent changes in observed Cotton effects as a result of changes in the degree of overlap of adjacent bands. However, it is possible that a given solvent might alter the distribution of conformers in the case of conformationally labile molecules such as those under consideration here. Such shifts in the equilibrium between conformers could lead to significant changes in the CD since the observed spectrum represents a weighted sum of the spectra of the specific conformers which are present.

Previous investigations by others have clearly indicated that there are at least two electronic transitions associated with the secondary amide chromophore, which occur in the region between 230 and 185 nm. One of these transitions, which exhibits very low absorbance and which undergoes red shifts as the solvent polarity is decreased, has been assigned to the magnetically allowed  $n-\pi^*$  transition.<sup>56,71</sup> A second band, which occurs around 186–188 nm in aqueous solution and which is strongly allowed, has been assigned to the  $\pi-\pi^*$  transition.<sup>55</sup>

Absorption, ORD, and CD studies have indicated that the optical rotatory properties of dipeptides in the region above 180 nm may be considered to arise from three Cotton effects: one band arising from the superposition of the  $n-\pi^*$  transitions of both amide groups, and a couplet which arises from the splitting of the degenerate  $\pi-\pi^*$  transitions. In practice, it is not possible to obtain data below approximately 190 nm in most of the solvent systems which were employed in this investigation; hence only two of the Cotton effects were observable. However, the presence of a third Cotton effect is evident from the band shape of the lower energy component of the  $\pi-\pi^*$  couplet.

The CD spectra of NALANMA exhibited two Cotton effects in the UV region above 190 nm which were observed to be solvent sensitive. As the solvent polarity was increased the long-wavelength band, which occurs near 220 nm in nonpolar media, was observed to be negative and undergo a gradual blue shift and an apparent decrease in intensity. Thus, this Cotton effect was assigned to the  $n-\pi^*$  transition, which should occur in this wavelength region. The shorter wavelength Cotton effect is presumably the long-wavelength component of the  $\pi-\pi^*$  couplet. This band exhibits an apparent blue shift and a change in sign, from positive to negative, as the solvent polarity is increased. Although this band is not clearly resolved in dioxane, it can be inferred from the shape of the longer wavelength  $n-\pi^*$  Cotton effect that it must be positive.

These results are consistent with the data of other investigators.<sup>42–44,46–48</sup> They are also in agreement with the ORD studies by Schellman and Nielsen<sup>45,72</sup> on *N*-acetyl-L-alanine amide, which should be very similar to NALANMA, except for the fact that the former compound apparently gives rise to a positive  $n-\pi^*$  Cotton effect in water at 27 °C.

The CD spectra of NALANMA exhibited marked solvent and temperature effects. The spectra in nonpolar solvents at 27 °C revealed negative  $n-\pi^*$  Cotton effects and positive  $\pi-\pi^*$  couplets. The conformations that should give rise to such a pattern fall in the regions of Figure 5 which are shaded with lines of positive slope, so they should be the dominant species in nonpolar solutions. In polar solvents, a weakly negative  $n-\pi^*$  band and a negative  $\pi-\pi^*$  couplet were observed. This pattern corresponds to the crosshatched region of the map, so the conformers that fall within this region should be the predominant ones existing in polar media. The CD pattern in ethanol was observed to change from a negative  $n-\pi^*$  and negative  $\pi-\pi^*$  couplet at 27 °C to a positive  $n-\pi^*$  and a negative couplet at –48 °C, which is in agreement with the study which was carried out at –90 °C by Ivanov et al.<sup>48</sup> This corresponds to a shift of the major conformers from a crosshatched region to a region which is shaded with lines of negative slope in Figure 5.

Generally, the conformational distribution for these molecules has been predicted to be either of two types: (1) an equilibrium primarily between a  $C_7$  form ( $C_7^{eq}$  and/or  $C_7^{ax}$ ) and an extended form ( $C_5$  or a similar conformer) in the E or E\* region, with the  $C_7$  form dominating in nonpolar media and the extended form dominant in polar media,<sup>25–28,30–36,38,39,41</sup> (2) a statistical ensemble of several conformations, the distribution of which is affected by solvent polarity and temperature.<sup>29,37,40,42,47,48,69,70,73</sup>

If one assumes only  $C_5$  and  $C_7$  conformers are present, no single conformational energy method yields results which are capable of explaining the CD data of NALANMA for both polar and nonpolar media. Empirical conformational energy methods appear to yield results which correlate with data obtained for solutions in nonpolar solvents, but not polar solvents. Other conformational energy techniques, such as the PCIO and CNDO methods, seem to yield results which are inconsistent with the CD data which were determined in nonpolar media, but they can be consistent with data from polar media, depending upon the relative ratio of conformer population that is assumed. The EHT method failed to give results which were consistent with experiment for either medium.

The  $C_7$  form might be important in nonpolar systems because the intramolecular hydrogen bonds which give rise to this species should be stabilized in such solvent systems. Comparison of the theoretical results of Table III with the experimental data of Figure 1 suggests that the dominant  $C_7$  form should be the  $C_7^{eq}$  rather than the  $C_7^{ax}$ . A strong positive  $n-\pi^*$  band is universally predicted for the  $C_7^{ax}$  form, which is contrary to experiment, except at low temperature. In some cases, a strong negative  $\pi-\pi^*$  couplet is predicted as well, which also does not agree with experimental data for nonpolar systems at ambient temperature but is consistent with results obtained in ethanol at low temperature. Therefore, the results of the subzero temperature studies (positive  $n-\pi^*$ , negative couplet) are consistent with both  $C_7$  forms or only the  $C_7^{ax}$  conformer being present.

Comparative analysis also indicates that the prevalent open form does not appear to be a "classic"  $C_5$  conformer; i.e.,  $\phi = \psi = -180^\circ$ . The amount of the  $C_5$ -type species

present might be expected to increase as the polarity of the solvent system is increased, because the hydrogen bonds which stabilize the  $C_7$  form should be disrupted. Such an increase in the proportion of the  $C_5$  form might lead to a decrease in the rotatory strength for the  $\pi-\pi^*$  band, since this conformer lies very near a nodal line for the rotatory strength of this transition. However, exactly the opposite effect is observed, so  $C_5$ -type conformers with  $\phi-\psi$  coordinates lying in other areas of the E region, which predict sizeable negative rotatory strengths for the  $n-\pi^*$  and  $\pi-\pi^*$  transitions, would appear to be more likely.

Conformational energy procedures which yield statistical weights for ensembles of conformers enable one to calculate average CD curves from the results of this investigation, as shown in Figure 7. The theoretical CD spectra for NALANMA seem to agree only with experimental data determined in nonpolar solution, which is not surprising since most of the conformational energy calculations did not include solvent effects. Quantitative agreement is best in the case of the study by Lewis et al.,<sup>15</sup> but the results may be affected by values of the bandwidths which were employed in the calculation of the theoretical curves.

The conformational energy calculations of Lipkind et al.<sup>7</sup> as well as more recent studies<sup>47,73</sup> have attempted to include solvent effects. Hodes et al.<sup>73</sup> predict a decrease in the number of conformers falling within the C region and an increase in the population of the A, D, E, and F regions, with a new minimum falling in the F region. They also predict that the global minimum should fall in the E region. Madison et al.<sup>47</sup> predict a shift from  $C_7$  to right-handed  $\alpha$ -helical and poly(proline II) conformations, which implies a decrease in the population of the C region and an increase in the populations of the A and F regions. The A and F regions were predicted to contain conformers which should yield the correct sign pattern for the low-temperature studies in ethanol. On the other hand, portions of the D and E regions predict the correct sign patterns insofar as data for polar media are concerned.

Three Cotton effects are also observed in the CD spectra of NALSNMA. As in the case of NALANMA, these were assumed to be associated with the  $n-\pi^*$  and  $\pi-\pi^*$  transitions. The CD spectra for NALSNMA, in the various solvents which were employed, were somewhat similar to those obtained with NALANMA. However, the solvent dependence was not nearly as drastic. The differences which were observed could be accounted for almost solely by shifts in the wavelengths of the  $n-\pi^*$  transitions. The  $n-\pi^*$  transitions again exhibited blue shifts and decreases in intensity. The  $\pi-\pi^*$  couplet showed no change in sign on going from nonpolar solvents, such as acetonitrile and cyclohexane, to polar solvents, such as water, but rather exhibited a slight increase in intensity and an apparent blue shift as the solvent polarity increased. Data for triethyl phosphate and dioxane could be obtained at a sufficiently low wavelength to unambiguously determine the sign of the couplet. The fact that the observed changes were much less drastic suggests either a less mobile conformational distribution, or else the distributions of conformers which exist in the different solvent systems are made up of conformers which, although different, exhibit similar chiroptical properties.

For NALSNMA, the experimental CD spectra show a negative  $n-\pi^*$  Cotton effect and a negative  $\pi-\pi^*$  couplet for both polar and nonpolar media at all temperatures. All of the conformations which predict such a sign pattern fall in the crosshatched region of the submaps which are shown in Figure 6. The conformations which lie in this region are expected to be the major forms existing under the

experimental conditions which were employed. Note that the points representing the various conformations fall in, or very near, a crosshatched region regardless of which submap is used. This suggests that although the distribution of conformers might be solvent and temperature dependent, the observed CD pattern might be less sensitive to changes in both of these experimental variables, which is in agreement with experimental observations.

The changes in the CD spectra of NALSNMA which are observed upon going from polar to nonpolar solvents could be explained by a shift in equilibrium from certain  $C_5$ -type forms (in the E region) to certain  $C_7$  forms (in the C region). In fact, recent ECEPP conformational energy calculations by Zimmerman et al.<sup>14</sup> and Lewis et al.<sup>15</sup> indicate that three conformers which fall in the C, D, and E regions have the greatest statistical weights. However, as pointed out by Madison and Kopple,<sup>47</sup> this apparent agreement may be purely coincidental since similar changes are observed in the CD spectra of *N*-acetylproline *N*-methylamide, where such conformational transitions are impossible. The other methods give results consistent with experimental data only in nonpolar media.

The  $C_7^{eq}$  form is predicted to be the dominant folded form in all of the conformational energy calculations, and this is consistent with the results of this study. Furthermore, the extended conformer which is the most prevalent may not be the  $C_5$  species, which has a very small rotatory strength, but rather another open form with  $\phi-\psi$  coordinates which place it away from the nodal line in the crosshatched portion of the E or E\* region.

The theoretical CD curves, shown in Figure 8, which were determined by employing the statistical weights calculated by the conformational energy procedures indicate that the Lewis et al.<sup>15</sup> results again give a qualitatively accurate theoretical curve only when compared to the experimental data determined in nonpolar solutions. On the other hand, the Zimmerman et al.<sup>14</sup> distribution, as a result of the heavy weighting of its  $C_7^{eq}$  species, fails to yield a theoretical curve with the correct sign pattern for either nonpolar or polar solvents.

Conformational energy calculations which attempted to include the effect of solvent have recently been carried out for NALSNMA.<sup>73</sup> These calculations predicted a decrease in the populations of the C, E, and G regions upon hydration, with an increase in the populations of the A, D, F, and A\* regions. Furthermore, the global minimum was predicted to shift from the C to the D region. A marked increase in the number of energy minima, as compared to unsolvated species, was predicted. It may be significant that the D region predicts a CD sign pattern which is consistent with experimental data determined in polar media and at low temperatures in ethanol.

## Conclusions

The techniques which were used in this investigation have previously proved capable of accounting for the solution conformation of a number of sterically hindered model compounds.<sup>74-79</sup> The present study represents a more difficult challenge since these molecules are much more conformationally labile than those studied previously. Nevertheless, several significant conclusions can be drawn from the results of this investigation.

In the case of NALANMA, none of the conformational energy methods seemed to yield results which are completely consistent with the CD data for both polar and nonpolar media. Most of the conformational energy data seem to be consistent only with the CD spectra determined in nonpolar solvents. The available evidence seems to support the presence of greater numbers of the  $C_7^{eq}$  form

than the  $C_7^{ax}$ . Furthermore, if  $C_5$ -type conformers are present in significant numbers, they must be species which would lie in the crosshatched portion of the E region of Figure 5.

The CD spectra of NALSNMA showed less drastic solvent and temperature effects than the spectra of NALANMA. However, this does not necessarily imply that the former molecule is less conformationally labile than the latter. It is quite possible that there are significant changes in the conformational distribution from one solvent to another, with these different distributions having very similar chiroptical properties. Again, however, the results of few of the conformational energy calculations were consistent with the CD data for both polar and nonpolar solvents. As in the case of NALANMA the  $C_7^{eq}$  and an extended form other than the "classic"  $C_5$  form appear to be the species most likely to be present in large numbers.

In summary, contrary to some earlier reports it seems very unlikely that the results of this investigation can be explained on the basis of an equilibrium between only two significant conformers, which is in agreement with several more recent experimental studies as well as many of the conformational energy calculations. With the possible exception of the ECEPP calculations for NALSNMA, most conformational energy methods have given results which are consistent with only CD data determined for nonpolar media. Thus, it seems obvious that solvent effects must be included in any calculations which attempt to calculate the conformational energy surface for molecules in polar media. Whatever type of conformational energy calculations are carried out and whatever assumptions are made regarding the number and nature of the conformational species which are present in a given medium, the results should yield a theoretical CD spectrum which is consistent with the results of this investigation.

**Acknowledgment.** The support of the National Institute of General Sciences of the National Institutes of Health through Grant GM-18092 is gratefully acknowledged. Equipment purchased with funds from Biomedical Sciences Support Grant S04-RR07099 was utilized in this research.

## References and Notes

- Popov, E. M.; Lipkind, G. M. *Mol. Biol.* 1971, 5, 624–36.
- Brant, D. A.; Miller, W. G.; Flory, P. J. *J. Mol. Biol.* 1967, 23, 47–65.
- Popov, E. M.; Lipkind, G. M.; Arkhipova, S. F.; Dashevskii, V. G. *Mol. Biol.* 1968, 2, 622–30.
- Liquori, A. M. *Q. Rev. Biophys.* 1969, 2, 65–92.
- Gibson, K. D.; Scheraga, H. A. *Biopolymers* 1966, 4, 709–12.
- Crippen, G. M.; Scheraga, H. A. *Proc. Natl. Acad. Sci. U.S.A.* 1969, 64, 42–9.
- Lipkind, G. M.; Arkhipova, S. F.; Popov, E. M. *Zh. Strukt. Khim.* 1970, 11, 121–6.
- Momany, F. A.; McGuire, R. F.; Yan, J. F.; Scheraga, H. A. *J. Phys. Chem.* 1971, 75, 2286–97.
- Govil, G. *J. Indian Chem. Soc.* 1971, 48, 731–7.
- Hoffmann, R.; Imamura, A. *Biopolymers* 1969, 7, 207–13.
- Momany, F. A.; McGuire, R. F.; Yan, J. F.; Scheraga, H. A. *J. Phys. Chem.* 1970, 74, 2424–35.
- Maigret, B.; Pullman, B.; Dreyfus, M. *J. Theor. Biol.* 1970, 26, 321–33.
- Maigret, B.; Pullman, B.; Perahia, D. *J. Theor. Biol.* 1971, 31, 269–85.
- Zimmerman, S. S.; Pottle, M. S.; Némethy, G.; Scheraga, H. A. *Macromolecules* 1977, 10, 1–9.
- Lewis, P. N.; Momany, F. A.; Scheraga, H. A. *Isr. J. Chem.* 1973, 11, 121–52.
- Ponnuswamy, P. K.; Sasisekharan, V. *Biopolymers* 1971, 10, 565–82.
- Govil, G.; Saran, A. *J. Chem. Soc., Faraday Trans. 2* 1972, 1176–80.
- Perahia, D.; Maigret, B.; Pullman, B. *Theor. Chim. Acta* 1970, 19, 121–34.
- Pullman, B.; Maigret, B.; Perahia, D. *Theor. Chim. Acta* 1970, 18, 44–56.
- Perahia, D.; Pullman, B.; Claverie, P. *Int. J. Quantum Chem.* 1972, 6, 337–45.
- Perahia, D. Ph.D. Thesis, University of Paris VI, 1971, quoted in: Pullman, B.; Maigret, B. In "Conformation of Biological Molecules and Polymers"; Bergmann, E. D., Pullman, B., Eds.; Academic Press: New York, 1973; pp 13–35.
- Govil, G.; Saran, A. *J. Chem. Soc. A* 1971, 3624–7.
- Smolikova, J.; Vitek, A.; Blaha, K. *Collect. Czech. Chem. Commun.* 1971, 36, 2474–85.
- Marraud, M. Ph.D. Thesis, University of Nancy, 1971, quoted in: Pullman, B.; Maigret, B. In "Conformation of Biological Molecules and Polymers"; Bergmann, E. D.; Pullman, B., Eds.; Academic Press: New York, 1973; pp 13–35.
- Neel, J. *Pure Appl. Chem.* 1972, 31, 201–25.
- Cung, M. T.; Marraud, M.; Neel, J. In "Conformation of Biological Molecules and Polymers"; Bergmann, E. D., Pullman, B., Eds.; Academic Press: New York, 1973; pp 69–83.
- Marraud, M.; Neel, J. *J. Chim. Phys.* 1972, 69, 835–40.
- Marraud, M.; Neel, J.; Avignon, M.; Huong, P. V. *J. Chim. Phys. Physicochim.* 1970, 67, 959–64.
- Efremov, E. S.; Senyavina, L. B.; Zheltova, V. N.; Ivanova, A. G.; Kostetskii, P. V.; Ivanov, V. T.; Popov, E. M.; Ovchinnikov, Yu. A. *Khim. Prir. Soedin.* 1973, 9, 322–38.
- Avignon, M.; Huong, P. V. *Biopolymers* 1970, 9, 427–32.
- Avignon, M.; Huong, P. V.; Lascombe, J.; Marraud, M.; Neel, J. *Biopolymers* 1969, 8, 69–89.
- Mizushima, S.; Shimanouchi, T.; Tsuboi, M.; Arakawa, T. *J. Am. Chem. Soc.* 1957, 79, 5357–61.
- Grenie, Y.; Avignon, M.; Garrigou-Lagrange, C. *J. Mol. Struct.* 1975, 24, 293–317.
- Avignon, M.; Lascombe, J. In "Conformation of Biological Molecules and Polymers"; Bergmann, E. D., Pullman, B., Eds.; Academic Press: New York, 1973; pp 97–105.
- Pullman, B.; Pullman, A. *Adv. Protein Chem.* 1974, 28, 347–526.
- Bystrov, V. F.; Portnova, S. L.; Tsetlin, V. I.; Ivanov, V. T.; Ovchinnikov, Y. A. *Tetrahedron* 1969, 25, 493–515.
- Ivanov, V. T.; Kostetskii, P. V.; Balashova, T. A.; Portnova, S. L.; Efremov, E. S.; Ovchinnikov, A. Yu. *Khim. Prir. Soedin.* 1973, 9, 339–48.
- Avignon, M.; Garrigou-Lagrange, C.; Bothorel, P. *Biopolymers* 1973, 12, 1651–69.
- Koyama, Y.; Uchida, H.; Oyama, S.; Iwaki, T.; Harada, K. *Biopolymers* 1977, 16, 1795–813.
- Efremov, E. S.; Kostetskii, P. V.; Ivanov, V. T.; Popov, E. M.; Ovchinnikov, Yu. A. *Khim. Prir. Soedin.* 1973, 9, 348–54.
- Weiler-Feilchenfeld, H.; Singerman, A.; Bergmann, E. D. In "Conformation of Biological Molecules and Polymers"; Bergmann, E. D., Pullman, B., Eds.; Academic Press: New York, 1973; pp 87–95.
- Ivanov, V. T.; Kostetskii, P. V.; Mescheryakova, E. A.; Efremov, E. S.; Popov, E. M.; Ovchinnikov, Yu. A. *Khim. Prir. Soedin.* 1973, 9, 363–78.
- Johnson, W. C.; Tinoco, I. *J. Am. Chem. Soc.* 1972, 94, 4389–90.
- Crippen, G. M.; Yang, J. T. *J. Phys. Chem.* 1974, 78, 1127–30.
- Nielsen, E. B.; Schellman, J. A. *Biopolymers* 1971, 10, 1559–81.
- Cann, J. R. *Biochemistry* 1972, 11, 2645–59.
- Madison, V.; Kopple, K. D. *J. Am. Chem. Soc.* 1980, 102, 4855–63.
- Ivanov, V. T.; Filatova, M. P.; Reissman, Z.; Reutova, T. O.; Chekhlyatva, N. M. *Bioorg. Khim.* 1977, 3, 1157–68.
- Bayley, P. M.; Nielsen, E. B.; Schellman, J. A. *J. Phys. Chem.* 1969, 73, 228–43.
- Applewhite, T. H.; Niemann, C. *J. Am. Chem. Soc.* 1959, 81, 2208–13.
- Zahn, H.; Reinert, G. *Z. Physiol. Chem.* 1968, 349, 608–10.
- Goux, W. J.; Hooker, T. M., Jr. *J. Am. Chem. Soc.* 1980, 102, 7080–7.
- Hooker, T. M., Jr.; Schellman, J. A. *Biopolymers* 1970, 9, 1319–48.
- Nielsen, E. B.; Schellman, J. A. *J. Phys. Chem.* 1967, 71, 2297–304.
- Peterson, D. L.; Simpson, W. T. *J. Am. Chem. Soc.* 1957, 79, 2375–82.
- Schellman, J. A.; Nielsen, E. B. *J. Phys. Chem.* 1967, 71, 3914–21.
- Carpenter, G. B.; Donohue, J. *J. Am. Chem. Soc.* 1950, 72, 2315–28.
- Frey, M. N.; Lehmann, M. S.; Koetzle, T. F.; Hamilton, W. C. *Acta Crystallogr., Sect. B* 1973, B29, 876–84.

- (59) Simpson, H. J.; Marsh, R. E. *Acta Crystallogr.* **1966**, *20*, 550-5.  
 (60) Pauling, L. "The Nature of the Chemical Bond", 3rd ed.; Cornell University Press: Ithaca, N.Y., 1960.  
 (61) IUPAC-IUB Commission on Biochemical Nomenclature *Biochemistry* **1970**, *9*, 3471-9.  
 (62) Poland, D.; Scheraga, H. A. *Biochemistry* **1967**, *6*, 3791-800.  
 (63) Del Re, G. *J. Chem. Soc.* **1958**, 4031-40.  
 (64) Del Re, G. *Theor. Chim. Acta* **1963**, *1*, 188-97.  
 (65) Del Re, G.; Pullman, B.; Yonezawa, T. *Biochim. Biophys. Acta* **1963**, *75*, 153-82.  
 (66) Berthod, H.; Pullman, A. *J. Chim. Phys.* **1965**, *62*, 942-6.  
 (67) Efremov, E. S.; Kostetskii, P. V.; Ivanov, V. T.; Popov, E. M.; Ovchinnikov, Yu. A. *Khim. Priro. Soedin.* **1973**, *9*, 354-63.  
 (68) Pullman, B.; Maigret, B. In "Conformation of Biological Molecules and Polymers"; Bergmann, E. D.; Pullman, B., Eds.; Academic Press: New York, 1973; p 13-35.  
 (69) Koyama, Y.; Uchida, H.; Oyama, S.; Iwaki, T.; Harada, K. *Biopolymers* **1977**, *16*, 1795-813.  
 (70) Maxfield, F. R.; Leach, S. J.; Stimson, E. R.; Powers, S. P.; Scheraga, H. A. *Biopolymers* **1979**, *18*, 2507-21.  
 (71) Bayliss, N. S.; McRae, E. G. *J. Phys. Chem.* **1954**, *58*, 1002-6, 1006-11.  
 (72) Schellman, J. A.; Nielsen, E. B. "Conformations of Biopolymers"; Ramachandran, G. N., Ed.; Academic Press: New York, 1967; pp 109-22.  
 (73) Hodes, Z. I.; Némethy, G.; Scheraga, H. A. *Biopolymers* **1979**, *18*, 1565-610.  
 (74) Snow, J. W.; Hooker, T. M., Jr. *J. Am. Chem. Soc.* **1974**, *96*, 7800-6.  
 (75) Snow, J. W.; Hooker, T. M., Jr. *J. Am. Chem. Soc.* **1975**, *97*, 3506-11.  
 (76) Snow, J. W.; Hooker, T. M., Jr. *Biopolymers* **1977**, *16*, 121-42.  
 (77) Goux, W. J.; Kadesch, T. R.; Hooker, T. M., Jr. *Biopolymers* **1976**, *15*, 977-97.  
 (78) Goux, W. J.; Cooke, D. B.; Rodriguez, R. E.; Hooker, T. M., Jr. *Biopolymers* **1974**, *13*, 2315-29.  
 (79) Grebow, P. E.; Hooker, T. M., Jr. *Biopolymers* **1975**, *14*, 1863-83.

## Notes

### Relationship between the Rotational Isomeric State and Wormlike Chain Models

MARC L. MANSFIELD

Department of Chemistry, Colorado State University, Fort Collins, Colorado 80523. Received June 8, 1981

Some interest has been shown in relating the Kratky-Porod wormlike chain model<sup>1,2</sup> to the rotational isomeric state (RIS) model<sup>3</sup> or to real polymer molecules in solution. Maeda, Saitō, and Stockmayer<sup>4</sup> demonstrated that a relationship existed between RIS and wormlike chains. They defined a "shift factor"  $f$ , given by  $n = fL/2a$  for  $n$ , the number of bonds of the RIS chain, and  $L$  and  $a$ , the contour length and persistence length, respectively, of the wormlike chain. They showed that for appropriate values of  $f$ , one could obtain very good agreement between both the second and fourth moments of the end-to-end vector of a number of sufficiently long RIS and wormlike chains. However, they were unable to give general rules for computing  $f$  and resorted finally to curve fitting. Along a somewhat different line, Yamakawa and co-workers<sup>5-8</sup> have compared wormlike chains to real chain molecules in solution and presented rules for determining the shift factor from various experimental properties. Recently, good agreement has been demonstrated<sup>9</sup> between certain RIS and wormlike star molecules. Mattice<sup>10</sup> examined a number of star molecules, finding many for which such agreement was lacking, and concluded that agreement was usually obtained for stars of large characteristic ratio. In this note, we give precise rules for the selection of the shift factor of Maeda et al.<sup>4</sup> for agreement between the second moments of wormlike and RIS chains. As has been recognized,<sup>4,10</sup> a good understanding of the relationship between the two models is desirable because of the relative simplicity of the wormlike model.

Two-bond correlations in a long RIS chain with all bonds identical can be written (cf. eq IV.16 of ref 3)

$$\langle \mathbf{l}_i \cdot \mathbf{l}_{i+j} \rangle = l^2 Z^{-1} \mathbf{L} \mathbf{M}^j \mathbf{R} \quad (1)$$

where  $\mathbf{L}$ ,  $\mathbf{R}$ , and  $\mathbf{M}$  are row, column, and square matrices, respectively, given by

$$\mathbf{L} = \mathbf{J} \cdot \mathbf{U}^{i-2} (\mathbf{E}_v \otimes \hat{\mathbf{l}}^T) \quad (2)$$

$$\mathbf{M} = (\mathbf{U} \otimes \mathbf{E}_3) \|\mathbf{T}\| \quad (3)$$

$$\mathbf{R} = (\mathbf{E}_v \otimes \hat{\mathbf{l}}) \mathbf{U}^{n-j-i} \mathbf{J} \quad (4)$$

where  $\hat{\mathbf{l}} = \mathbf{l}/l$  and all other notation follows ref 3. We set  $1 \ll i \leq i+j \ll n$  so that the dominant eigenvalue,  $\lambda_1$ , of  $\mathbf{U}$  determines the partition function,  $Z$ :<sup>3</sup>

$$Z = \Gamma_1 \lambda_1^{n-2} \quad (5)$$

where  $\Gamma_1$  is defined in ref 3.

Let  $\mathbf{A}$  be the diagonalizing similarity transformation of  $\mathbf{M}$ . ( $\mathbf{A}^{-1} \mathbf{M} \mathbf{A}$  is diagonal with elements  $m_\mu$ .) Then

$$\langle \mathbf{l}_i \cdot \mathbf{l}_{i+j} \rangle = l^2 Z^{-1} \sum_{\mu} \Omega_{\mu} m_{\mu}^j \quad (6)$$

where

$$\Omega_{\mu} = \sum_{\sigma\rho} L_{\sigma} A_{\sigma\mu} A_{\mu\rho}^{-1} R_{\rho} \quad (7)$$

Because we have assumed that  $1 \ll i$  and  $i+j \ll n$ , all of the  $i$  and  $j$  dependence in  $\mathbf{L}$  and  $\mathbf{R}$  appears in the factors  $\lambda_1^{i-2}$  and  $\lambda_1^{n-j-i}$ , respectively, so the  $i$  and  $j$  dependence of  $\Omega_{\mu}$  can be expressed as

$$\Omega_{\mu} = \lambda_1^{n-j-2} \Pi_{\mu} \quad (8)$$

Then

$$\langle \mathbf{l}_i \cdot \mathbf{l}_{i+j} \rangle = l^2 \sum_{\mu} K_{\mu} \alpha_{\mu}^j \quad (9)$$

for  $K_{\mu} = \Pi_{\mu}/\Gamma_1$  and  $\alpha_{\mu} = m_{\mu}/\lambda_1$ . The corresponding expression for a wormlike chain of persistence length  $a$  is<sup>2</sup>

$$\langle \mathbf{u}(s) \cdot \mathbf{u}(s') \rangle = \exp(-|s' - s|/a) \quad (10)$$

for  $\mathbf{u}(s)$  the unit vector tangent to the wormlike curve at the contour distance  $s$ . On the basis of the above, therefore, a sufficient condition for good agreement between the two models is the following:

(1) One of the  $K_{\mu}$  is dominant, and (11a)

(2) the associated  $\alpha_{\mu}$  is near 1 (11b)

Condition 11a ensures that a single exponential will dominate in eq 9 and condition 11b ensures that  $\sum_j \alpha_{\mu}^j \simeq \int dx \exp(x \ln \alpha_{\mu})$ . Although condition 11 will certainly lead to good agreement between the two models, we actually find that agreement is more general.

The second moment of a wormlike chain of contour length  $L$  is given by<sup>2,3</sup>